Variation Simulation of Rigid Bodies with Contact Representation

Available online at www.sciencedirect.com

ScienceDirect

Procedia CIRP 145 (2026) 79–84

www.elsevier.com/locate/procedia

19th CIRP Conference on Computer Aided Tolerancing

Variation Simulation of Rigid Bodies with Contact Representation

Roham Sadeghi Tabar*, Lars Lindkvist, Kristina Wärmefjord, Rikard Söderberg

[a]*Department of Industrial and Materials Science, Chalmers University of Technology, SE-412 96 Gothenburg, Sweden*

* Corresponding author. Tel.: +46-31-772-6745 . *E-mail address:* rohams@chalmers.se

Abstract

Variation simulation is widely used for statistical quality control of mechanical assemblies subject to geometric variation. A major challenge lies in accurately modeling contact interactions between rigid components to consistently configure the rigid bodies. This paper presents a Monte-Carlo variation simulation framework that explicitly incorporates rigid-body normal contact using unilateral non-penetration constraints. The proposed method is applied to two reference assemblies and compared against a conventional contactless variation simulation approach. Results show that enforcing contact constraints significantly alters the predicted assembly behavior by reducing the 6σ spread of critical measurement points, while introducing a directional bias along the contact normal reflected by a shift in the mean displacement. These findings demonstrate that contact modeling plays a critical role in realistic variation simulation. The proposed framework provides a physically consistent and computationally efficient basis for contact-aware tolerance analysis of rigid-body assemblies.

Peer-review under responsibility of the scientific committee of the 19th CIRP Conference on Computer-Aided Tolerancing (CAT 2026)

Keywords: Geometric Variation Simulation; Contact Model, Geometric Quality, Tolerance

1. Introduction

Mechanical products increasingly rely on tight geometric interactions and clearances on interfaces, locating schemes, and functional surfaces to achieve geometric and functional targets [1, 2, 3]. In such systems, small manufacturing variation can shift the realized contact topology. The contact topology defines which faces touch, where they touch, and what normal load contact interfaces have. Variation in the contact interface produces large downstream effects on functional key characteristics (KCs) such as gaps, flushes, or clearances [4]. This sensitivity is amplified in rigid or non-rigid assemblies where geometry governs closure and loads [4]. As a result, modern tolerance engineering must couple (i) unambiguous specification of allowable geometric variation, (ii) statistical models of manufactured populations, and (iii) physically consistent contact models that convert geometric realizations into assembly responses.

1.1. Geometric tolerancing as a product definition language

Geometric dimensioning and tolerancing (GD&T), i.e., the ISO GPS system, provides the formal language for communicating allowable variations in form, orientation, and location relative to datums and datum systems [5]. International practice is largely anchored by GD&T standard frameworks that formalizes specification and verification concepts, operators, uncertainties, and the link between design intent and measurement. From a functional perspective, tolerances are not merely documentation artifacts; they encode constraints on the admissible set of part geometry models and derived features that the assembly process will attempt to connect [6]. The same nominal CAD assembly may therefore admit many feasible realized assemblies, depending on how the specified tolerance and how contacts and constraints resolve. Therefore, a propagation model that maps a population of part deviations to a distribution of functional KCs under realistic assembly conditions is essential.

1.2. Tolerance analysis

Classical tolerance stack-up approaches are often categorized as worst-case or statistical. Worst-case methods guarantee functional and aesthetic specifications but can overestimate variation when multiple independent contributors rarely align at the extremes. Statistical methods, including root sum square approximations for linearized stack-ups and more general simulation-based techniques, aim to predict realistic yield for manufactured populations while enabling cost-performance trade-offs [7, 8]. Surveys of tolerance analysis for mechani-

2212-8271 © 2026 The Authors. Published by Elsevier B.V.

Peer-review under responsibility of the scientific committee of the 19th CIRP Conference on Computer-Aided Tolerancing (CAT 2026)
10.1016/j.procir.2026.03.148

cal assemblies highlight both the practical importance and the methodological diversity of this field, spanning linearized sensitivity methods, nonlinear geometric constraint solving, and sampling-based simulation [8, 9]. However, many real assemblies are nonlinear, contact engagement changes the interface conditions, constraint sets can change with small perturbations, and resulting KCs may be non-smooth functions of the underlying deviations [10]. Linearized stack-ups and Gaussian assumptions can fail to capture true contact behavior that drives scrap and rework risk. This motivates statistical variation simulation approaches that evaluate the assembly response under many sampled realizations, directly accounting for contact transitions and constraint activation.

1.3. Statistical variation simulation

Monte-Carlo (MC) simulation is widely used in statistical tolerance analysis because it handles arbitrary input distributions [2]. The general workflow samples part-level deviations from specified or empirically fitted distributions, assembles the parts under modeled constraints, and records the resulting functional KC; repeating this over many trials yields an estimate of the KC distribution and the probability of meeting the requirements [1]. Literature describes MC tolerance analysis as a practical baseline against which alternative uncertainty propagation methods [9] are compared. This approach has also been extended for variation simulation of defomrable parts [11]. Several studies have been performed analyzing the impact of contributing parameters, *i.e.*, clamping [12], spot welding, sequence of operations [13], continuous welding [14] and matching [15]. The digital twin perspective has also emerged from this approach [1, 16, 17]. Despite its conceptual simplicity, MC-based tolerance analysis relies on the fidelity of two modeling layers:

- Variation modeling: how GD&T requirements are converted into realizations of surfaces and features consistent with standard semantics.
- Assembly variation: how the realized parts are brought into an assembled configuration, particularly when closure is governed by unilateral contacts and datum constraints.

The second layer is frequently the limiting factor: if contact is not treated, predicted variation and sensitivity can be biased, especially for tight clearances and complex datum schemes.

1.4. Contact models for rigid-body assembly

Contact between solid bodies is classically studied in elastic contact mechanics, originating with Hertz's solution for elastic bodies and later consolidated in canonical treatments [18]. For tolerance analysis of stiff assemblies and 3-2-1 locating systems, it is often appropriate to adopt a rigid-body, frictionless, unilateral contact where bodies are treated as rigid, tangential forces are neglected, and the normal interaction enforces non-penetration contact reactions. This approach has been adapted initially for elastic sheet metal assemblies [10, 19]. Here, geometric closure is prioritized, and contact topology over local elastic deformation makes it attractive for fast, repeated evaluation inside MC simulations.

Rigid unilateral contact is naturally expressed by a non-negative normal gap, and a non-negative normal contact reaction cannot be both positive simultaneously. This is also referred to as the complementarity conditions. Time-stepping methods for rigid-body dynamics popularized such complementarity-based contact formulations and robust numerical schemes, including implicit approaches that handle simultaneous contacts [20]. For unilateral contact specifically, complementarity-based and time-stepping approaches have been analyzed and applied in the literature [21, 22]. The resulting mathematical problems often reduce to linear complementarity problems (LCPs) or closely related convex programs, depending on modeling choices. Within a tolerance analysis context, the key benefit of complementarity-based normal contact models is physical consistency, as they enforce non-penetration, correctly admit separation, and produce compressive-only reactions. These properties are crucial when small geometric deviations decide whether a locator engages, whether a gap closes, or which subset of surfaces carries load, all common scenarios in locating-based assembly variation simulation. Unlike contact-less rigid-body variation simulation and broader contact formulations for rigid or compliant assembly analysis, the proposed method explicitly resolves contact within each Monte-Carlo realization and is tailored for repeated large-batch tolerance-analysis evaluations that reveal the effect of contact on predicted KC distributions.

1.5. Scope of the paper

Motivated by the above, this paper focuses on an assembly analysis framework that combines: (i) consistent geometric tolerancing concepts as the specification language. (ii) MC statistical variation simulation to capture nonlinear and part and assembly variation mappings. (iii) a rigid-body unilateral normal contact model that resolves interpenetration through a convex quadratic correction step for each realization.

2. Methods

A rigid-body assembly composed of multiple parts subject to geometric variation is the problem under study. Assembly variation is evaluated through a MC simulation in which random rigid-body perturbations are applied to each part and subsequently corrected by enforcing normal contact constraints. The objective is to determine physically admissible, non-penetrating configurations and to quantify the resulting statistical variation of geometric features. The overview of the approach is presented in Fig. 1.

2.1. Monte-Carlo sampling of rigid-body variation

Geometric variation is modeled by sampling rigid-body motions of the parts. For each MC realization k, a rigid transfor-

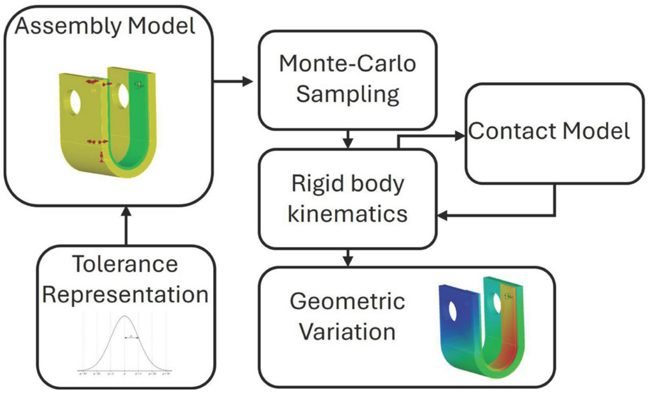

Fig. 1: Schematic view of the proposed approach

mation is drawn for each part,

$$\mathbf{x}^{(k)} = \mathbf{R}^{(k)}\mathbf{x}_0 + \mathbf{t}^{(k)}, \tag{1}$$

where $\mathbf{R}^{(k)}$ is a 3×3 orthogonal rotation matrix and $\mathbf{t}^{(k)} \in \mathbb{R}^3$ denote the sampled translation and $\mathbf{x}_0$ is a point in the nominal configuration. The distribution of $(\mathbf{R}^{(k)}, \mathbf{t}^{(k)})$ is defined by the tolerance model, *e.g.*, normal distributions on translation components and small-angle rotations. Each realization represents an unconstrained assembly configuration prior to contact solution and is referred to as the raw state.

2.2. Contact discretization

Normal contact between rigid bodies is represented using a point-to-surface discretization. A finite set of candidate contact pairs is constructed from the nominal geometry by:

1. selecting surface points on the potentially moving body, *i.e.* , mesh vertices.
2. projecting these points onto the opposing body surface, and
3. retaining pairs within a distance threshold.

Each contact pair i is characterized by a point on the moving body $\mathbf{P}_i^{\mathrm{m}}$, a corresponding point on the reference body $\mathbf{P}_i^{\mathrm{r}}$, and an outward unit normal $\mathbf{n}_i^{\mathrm{r}}$ at the reference surface. This discretization is fixed for all MC realizations and provides a linearized approximation of the potential contact region. In this perspective, the non-ideal shapes, *i.e*, skin models, are only necessary on the discretized contact set, modifying the corresponding nominal vertices. The schematic view of this discretization is shown in Fig. 2. In this approach, all potential contacting surfaces may be preselected as contact areas to be included in the analysis. Iterative contact search steps may also be integrated into the approach to account for newly emerging contact regions resulting from large perturbations.

2.3. Rigid-body kinematics and gap function

For a given MC realization, the global positions of the contact points for the reference and moving parts are presented as:

$$\mathbf{x}_i^{\mathrm{r}} = \mathbf{R}_{\mathrm{r}}\mathbf{P}_i^{\mathrm{r}} + \mathbf{t}_{\mathrm{r}}, \qquad \mathbf{x}_i^{\mathrm{m}} = \mathbf{R}_{\mathrm{m}}\mathbf{P}_i^{\mathrm{m}} + \mathbf{t}_{\mathrm{m}}. \tag{2}$$

The relative displacement vector at contact i is

$$\mathbf{u}_{0,i} = \mathbf{x}_i^{\mathrm{m}} - \mathbf{x}_i^{\mathrm{r}}. \tag{3}$$

The contact normal is rotated into the global frame as

$$\mathbf{n}_i = \frac{\mathbf{R}_{\mathrm{r}}\,\mathbf{n}_i^{\mathrm{r}}}{\|\mathbf{R}_{\mathrm{r}}\,\mathbf{n}_i^{\mathrm{r}}\|}. \tag{4}$$

The normal gap is defined as

$$g_{0,i} = \mathbf{n}_i^{\top}\mathbf{u}_{0,i}, \tag{5}$$

where $g_{0,i} < 0$ indicates penetration. This definition of the normal gap function is also visualized in Fig. 2. In the presence of tangential resistance, this formulation would need to be extended to account for frictional forces and potentially dynamic displacement responses.

2.4. Linearized contact correction

The moving body is corrected by a small rigid-body increment

$$\Delta\mathbf{q} = \left[\Delta t_x\ \Delta t_y\ \Delta t_z\ \omega_x\ \omega_y\ \omega_z\right]^{\top}, \tag{6}$$

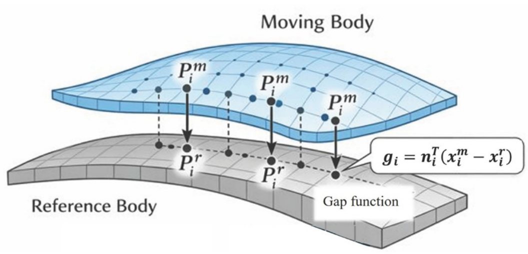

Fig. 2: schematic view of the contact discretization

where $\Delta\mathbf{t}$ is a translation and $\boldsymbol{\omega}$ a small rotation vector. The induced displacement at contact i is linearized as

$$\Delta\mathbf{u}_i = \mathbf{B}_i\Delta\mathbf{q}, \tag{7}$$

where $\mathbf{B}_i \in \mathbb{R}^{3\times6}$ is the rigid-body kinematic mapping constructed from the local position of $\mathbf{P}_i^{\mathrm{m}}$. The updated gap is then

$$g_i(\Delta\mathbf{q}) = \mathbf{n}_i^\top \left(\mathbf{u}_{0,i} + \mathbf{B}_i\Delta\mathbf{q}\right). \tag{8}$$

Only contacts with $g_{0,i}$ below a small tolerance are treated as active constraints.

2.5. Contact optimization problem

To enforce non-penetration while minimally perturbing the sampled configuration, the following convex quadratic program is solved [23]:

$$\min_{\Delta\mathbf{q}} \quad \frac{1}{2}\Delta\mathbf{q}^\top\mathbf{Q}\,\Delta\mathbf{q} \tag{9}$$

$$\text{s.t.} \quad g_i(\Delta\mathbf{q}) \geq 0, \qquad \forall i \in \mathcal{A}, \tag{10}$$

where $\mathcal{A}$ is the set of active contacts. The weighting matrix is chosen as

$$\mathbf{Q} = \sum_{i\in\mathcal{A}} \mathbf{B}_i^\top\mathbf{B}_i + \eta\mathbf{I}, \tag{11}$$

with $\eta > 0$ ensuring numerical stability. This formulation results in the smallest rigid-body correction that eliminates interpenetration. The problem is convex and is solved using a standard quadratic programming solver. The corrected rigid transform is obtained via a small-angle update,

$$\mathbf{R}_{\mathrm{m}}^{(\mathrm{corr})} = (\mathbf{I} + [\boldsymbol{\omega}]_\times)\mathbf{R}_{\mathrm{m}}, \qquad \mathbf{t}_{\mathrm{m}}^{(\mathrm{corr})} = \mathbf{t}_{\mathrm{m}} + \Delta\mathbf{t}. \tag{12}$$

Here $[\boldsymbol{\omega}]_\times$ denotes the skew-symmetric matrix associated with the rotation vector $\boldsymbol{\omega}$, such that $[\boldsymbol{\omega}]_\times\mathbf{v} = \boldsymbol{\omega}\times\mathbf{v}$. The associated skew-symmetric matrix $[\boldsymbol{\omega}]_\times \in \mathbb{R}^{3\times3}$, which represents the cross-product operator, is defined as

$$[\boldsymbol{\omega}]_\times = \begin{bmatrix} 0 & -\omega_z & \omega_y \\ \omega_z & 0 & -\omega_x \\ -\omega_y & \omega_x & 0 \end{bmatrix}. \tag{13}$$

2.6. Monte-Carlo statistics and variation fields

The above procedure is repeated independently for all MC realizations. For each realization, both the raw and the contact-corrected configurations are stored. For a set of evaluation points $\mathbf{v}_j$ attached to a body, the displacement in realization k is

$$\mathbf{u}_j^{(k)} = \left(\mathbf{R}^{(k)}\mathbf{v}_j + \mathbf{t}^{(k)}\right) - \mathbf{v}_j. \tag{14}$$

Statistical variation is quantified by computing sample means and standard deviations over all realizations. Results are reported as 6σ values of the displacement magnitude and of each Cartesian component, providing a spatial description of assembly-induced variation.

3. Method Evaluation

The proposed variational simulation (VS) and contact model method is applied to two reference assemblies, and the geometric variation is compared with the standard contactless method. The reference assemblies are described below.

3.1. Reference assemblies

The reference assembly 1 (RA 1) is a simple assembly of two blocks and is chosen for its simplicity and ability to visualize the contact modeling outcome. The assembly is visualized in Fig. 3a. The base part is $100 \times 50 \times 10$ mm, and the top part has a dimension of $50\times25\times10$ mm. The 3-2-1 locating scheme for each part is visualized with the thick arrows. The measurement point (KC) and its direction is also visualized with the local frame and its direction on the lower right corner of the top part. The predefined contact area is visualized with the grid on the interface of the two parts. Linear symmetric tolerance ranges of 10 mm have been applied to the positioning system of both parts, and a linear tolerance range of 1 mm is applied to the measurement point in the Z cartesian component. 1000 MC samples have been generated from these tolerances, and the variation on the geometry and the measurement point is analyzed.

The contact zone is discretized, and in total, 202 contact points are assigned to evaluate the gaps. The contact points are visualized in the Fig. 4. Furthermore, reference assembly 2 (RA 2), composed of two U-shaped plates with stamped holes, is analyzed for more complex contact interaction. The model, including the positioning points and the measurement point on the hole center, and 3000 defined contact pairs is visualized in Fig. 3b. Linear symmetric tolerance ranges of 5 mm have been applied to the positioning system, and 1000 samples have been analyzed.

3.2. Variation Simulation Results

The proposed contact model and VS method is applied to the reference assemblies, and the mean and geometric variation of

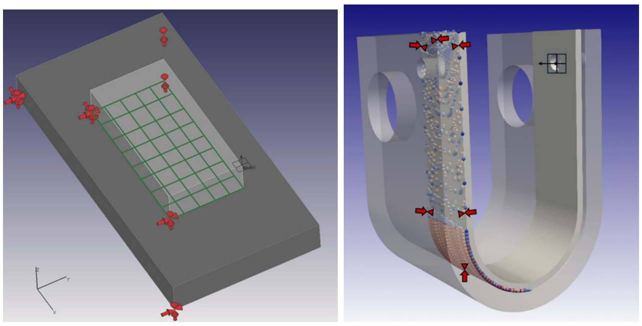

(a) Reference Assembly 1 (RA 1) (b) Reference Assembly 2 (RA 2)

Fig. 3: The reference assemblies and the contact area

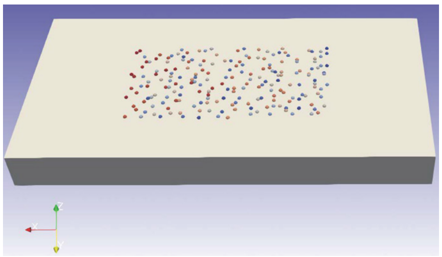

Fig. 4: Discretized contact area in RA 1

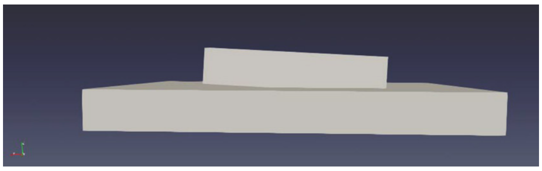

(a) Before contact

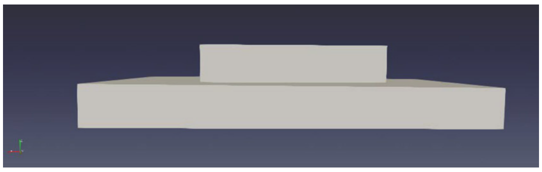

(b) After contact

Fig. 5: Reference Assembly deviation

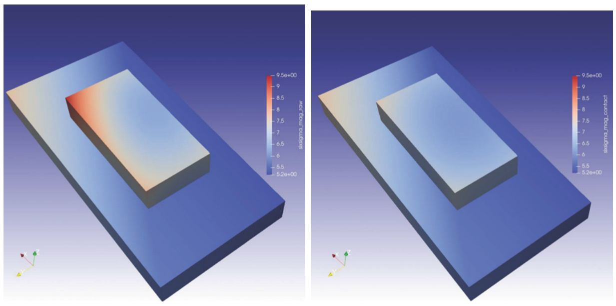

(a) Before contact (b) After contact

Fig. 6: Reference Assembly A variation. Colorplot scale range [5.2-9.5] mm

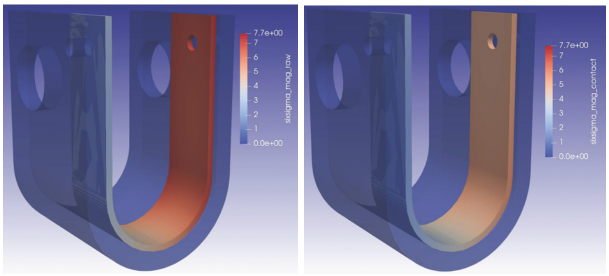

(a) Before contact (b) After contact

Fig. 7: Reference Assembly B variation. Colorplot scale range [0-7.7] mm

the magnitude of displacements of the overall geometry and the measurement point are studied and compared to the standard VS method. Fig. 5 visualizes the impact of the contact model on one MC instance in RA 1. In Fig. 5a, the reference contactless state is visualized, where interpenetration is allowed. The top part on the right side has penetrated the boundary of the base geometry. This interpenetrating configuration is physically prevented by the contact surface of the base part. After considering the contact interaction, the new deviation state is computed and visualized in Fig. 5b. The interpenetration between the two parts is modified and addressed in 5b.

Furthermore, the magnitude of the displacements over the 1000 MC sample is analyzed. Fig. 6a shows the propagation of the variation across both parts in RA 1, with a range of 5.2 to 9.5 mm across the samples. Fig. 6b presents the same analysis, presented in the same range, after considering the contact interactions. The maximum value of the sensitive area has been reduced by 19.72% due to contact interaction.

The measurement point analysis is performed, and the statistics summary is presented in Table 1. The measurement point is in the Z-direction, and the mean value over the 1000 samples is 0.06 mm in the contactless VS, and for the VS and contact method, this has been increased to 0.2734 mm. For the variation, the spread has been reduced by the contact interaction by 39%. The variance of the distribution has also been reduced by 62.9% due to the contact interactions. While contact constraints reduce the variance of the measured displacement, they introduce a directional bias by suppressing motion in the direction of penetration. As a result, the displacement distribution becomes truncated, increasing the mean value along the contact normal. By prohibiting interpenetration, contact constraints limit the range of admissible rigid-body motions, thereby reducing the spread of the displacement distribution and yielding a smaller 6σ value. For RA 2, the same overall trend is observed, confirming that the proposed method is not limited to the planar interface in RA 1. When contact is enforced, the predicted variation at the measurement point is reduced substantially, with the 6σ and the variance decreasing, Fig. 7. This indicates that, also for a more complex geometry with non-orthogonal contact interactions and a larger number of candidate contact pairs, unilateral contact constraints significantly restrict the admissible rigid-body motions, Fig. 7a and 7b. In contrast to RA 1, the mean value in RA 2 shifts in the negative direction, Table 1, which is explained by the orientation of the active contact normals and by the fact that only the inner part is subjected to variation while the outer part acts as the reference.

Table 1: Statistical results for the measurement point in RA 1 and RA 2

VS Measurement Statistics	Contactless RA 1	Contact RA 1	Contactless RA 2	Contact RA 2
Mean (mm)	0.0632	0.2734	-0.0014	-0.0664
6σ (mm)	16.1173	9.8223	12.5187	5.8544
Variance (mm^2)	7.2158	2.6799	4.3534	0.9521

4. Conclusion

This paper presented a rigid-body variation simulation framework that explicitly incorporates unilateral normal contact into MC–based tolerance analysis. The proposed approach formulates contact resolution as a convex quadratic optimization problem that enforces non-penetration while minimizing rigid-body correction, enabling robust and computationally efficient assembly simulation across large sample sets. The two reference assemblies demonstrated that neglecting contact interactions can lead to physically inconsistent assembly states with interpenetration and biased predictions of geometric variation. By enforcing normal contact constraints, the proposed method modified the admissible configuration space, resulting in physically realizable assemblies. The results showed a substantial reduction in geometric variation when contact was considered, with the 6σ spread of the measurement point reduced by approximately 39 to 53% compared to the contactless variation simulation. At the same time, contact introduced a directional bias along the contact normal, leading to a shift in the mean displacement as a consequence of unilateral constraints truncating the distribution of admissible motions. These findings confirm that contact modeling is a primary driver of assembly variation behavior in rigid assemblies where the locating scheme and tight clearances due to part variation are the main sources of variation. Although compliant contact formulations are highly relevant in assembly analysis, they are based on different mechanical assumptions and solution procedures; therefore, the present work does not include a direct quantitative comparison with such methods, but instead establishes a rigid-body contact-aware formulation as a basis for future extensions toward compliant assemblies.

Future work will focus on extending the proposed framework by incorporating tangential friction effects for more realistic modeling. Additionally, extending the formulation to include compliant contact behavior for analyzing deformable parts is also in the research plan.

Acknowledgments

This work was carried out at the Wingquist Laboratory within the Area of Advance Production at Chalmers, and supported by the Swedish Innovation Agency, Vinnova, through the project 2024-02505. The support is gratefully acknowledged.

References

[1] R. Söderberg, K. Wärmefjord, J. S. Carlson, L. Lindkvist, Toward a digital twin for real-time geometry assurance in individualized production, CIRP Annals 66 (1) (2017) 137 – 140.

[2] J. Camelio, S. J. Hu, D. Ceglarek, Modeling variation propagation of multi-station assembly systems with compliant parts, J. Mech. Des. 125 (4) (2003) 673–681.

[3] E. Morse, J.-Y. Dantan, N. Anwer, R. Söderberg, G. Moroni, A. Qureshi, X. Jiang, L. Mathieu, Tolerancing: Managing uncertainty from conceptual design to final product, CIRP Annals 67 (2) (2018) 695–717.

[4] G. Ungemach, F. Mantwill, Efficient consideration of contact in compliant assembly variation analysis, Journal of Manufacturing Science and Engineering 131 (1) (2008) 011005. doi:10.1115/1.3046133.

[5] Z. Humienny, State of art in standardization in gps area, CIRP Journal of Manufacturing Science and Technology 2 (1) (2009) 1–7. doi:https://doi.org/10.1016/j.cirpj.2009.06.007.

[6] M. Roth, A. Rezaei Aderiani, E. Morse, K. Wärmefjord, R. Söderberg, Closing gaps in the digital thread with the quality information framework (qif) standard for a seamless geometry assurance process, Computer-Aided Design 182 (2025) 103860. doi:https://doi.org/10.1016/j.cad.2025.103860.

[7] K. W. Chase, A. R. Parkinson, A survey of research in the application of tolerance analysis to the design of mechanical assemblies, Research in Engineering design 3 (1) (1991) 23–37.

[8] S. D. Nigam, J. U. Turner, Review of statistical approaches to tolerance analysis, Computer-Aided Design 27 (1) (1995) 6–15.

[9] Y. Cao, T. Liu, J. Yang, A comprehensive review of tolerance analysis models, The International Journal of Advanced Manufacturing Technology 97 (5) (2018) 3055–3085.

[10] R. S. Tabar, S. Lorin, L. Lindkvist, K. Wärmefjord, R. Söderberg, Robust contact computation in non-rigid variation simulation, Journal of Computing and Information Science in Engineering 24 (8) (2024) 081006.

[11] S. C. Liu, S. J. Hu, Variation simulation for deformable sheet metal assemblies using finite element methods, Journal of Manufacturing Science and Engineering 119 (3) (1997) 368–374.

[12] R. Sadeghi Tabar, H. Zheng, F. Litwa, K. Paetzold-Byhain, L. Lindkvist, K. Wärmefjord, R. Söderberg, Digital twin-based clamping sequence analysis and optimization for improved geometric quality, Applied Sciences 14 (2) (2024) 510.

[13] R. Sadeghi Tabar, K. Wärmefjord, R. Söderberg, L. Lindkvist, Critical joint identification for efficient sequencing, Journal of Intelligent Manufacturing 32 (2021) 769–780.

[14] R. Sadeghi Tabar, L. Lindkvist, K. Wärmefjord, P. Franciosa, D. Ceglarek, R. Söderberg, Enhancing welding geometric precision: analyzing the impact of weld path directions, sequences and locating schemes on displacement, Applied Sciences 14 (23) (2024) 11144.

[15] R. S. Tabar, K. Wärmefjord, R. Söderberg, Optimal part matching and joining sequence in non-rigid assemblies for improved geometric quality, Procedia CIRP 114 (2022) 141–146.

[16] R. Sadeghi Tabar, R. Söderberg, D. Ceglarek, P. Franciosa, L. Lindkvist, Augmented geometry assurance digital twin with physics-based incremental learning, CIRP Annals 74 (1) (2025) 151–155.

[17] B. Schleich, N. Anwer, L. Mathieu, S. Wartzack, Shaping the digital twin for design and production engineering, CIRP Annals 66 (1) (2017) 141–144.

[18] P. Wriggers, T. A. Laursen, Computational contact mechanics, Vol. 2, Springer Berlin, Heidelberg, 2006.

[19] B. Lindau, S. Lorin, L. Lindkvist, R. Söderberg, Efficient contact modeling in nonrigid variation simulation, Journal of Computing and Information Science in Engineering 16 (1) (2016) 011002.

[20] G. Gilardi, I. Sharf, Literature survey of contact dynamics modelling, Mechanism and machine theory 37 (10) (2002) 1213–1239.

[21] X. Yan, A. Ballu, Tolerance analysis using skin model shapes and linear complementarity conditions, Journal of Manufacturing Systems 48 (2018) 140–156.

[22] D. E. Stewart, J. C. Trinkle, An implicit time-stepping scheme for rigid